CHAPTER 36

Segmentation and Step-Overs Along Strike-Slip Fault Systems in the Inner California Borderlands: Implications for Fault Architecture and Basin Formation

Jillian M. Maloney[1], **and Neal W. Driscoll**[1]
[1]Scripps Institution of Oceanography, University of California at San Diego, 9500 Gilman Drive, La Jolla, CA 92093, USA
Jillian M. Maloney[2]
[2]Department of Geological Sciences, San Diego State University, San Diego, CA 92182-1020, USA, jmaloney@mail.sdsu.edu
Graham M. Kent[3], **and Jayne Bormann**[3]
[3]Nevada Seismological Laboratory, University of Nevada, Reno, Reno, NV 89557-0174, USA
Steve Duke[4], **and Thomas Freeman**[4]
[4]GeoPentech, Santa Ana, CA 92701, USA

ABSTRACT

Recent observations of compressional deformation in the inner California borderlands (ICB) offshore southern California have sparked debate over tectonic processes in the region. Two end-member models have been proposed to explain the young apparent compressional deformation observed in the ICB. One model invokes reactivation of detachment faults such as the Oceanside blind thrust (OBT) to explain the deformation and margin architecture (e.g., San Mateo/Carlsbad trends). In contrast, the other model explains this deformation by step-overs and trend changes along several north to northwest-oriented strike-slip fault systems. Reprocessed, industry multichannel seismic (MCS) reflection data were examined to characterize the geometry and linkage of faulting in the ICB. New observations gained from these data provide evidence that deformation in the ICB is more consistent with the step-over geometry and trend changes than a regional blind thrust model. For example, regions in the ICB exhibit both compressional and extensional structures across the margin, which are more readily explained by the strike-slip model. Localized transpression and transtension occurs as predicted at fault bends and step-overs in a strike-slip fault system. In addition, onlapping turbidite layers reveal that the deformation becomes stratigraphically younger towards the east, an observation that is inconsistent with a westward verging blind thrust fault system. Finally, rotational deformation previously attributed to a splay off the OBT instead appears to be a southward transported slide deposit. In summary, ICB tectonic deformation and margin architecture are best explained by step-overs along strike-slip fault systems. The lack of an OBT reduces the hazard for coastal regions in southern California because there would be no hangingwall effects and nearby slip rates would be reduced.

Introduction

Numerous onshore and offshore studies have vastly improved our understanding of the inner California borderlands (ICB) geology, fault structure, and recency of faulting (Darigo and Osborne, 1986; Hogarth et al., 2007; Kennedy and Clarke, 1999; Kennedy and Tan, 2005; Kennedy et al., 1975; Kennedy and Welday, 1980; Le Dantec et al., 2010; Legg, 1985; Legg and Kennedy, 1979; Lindvall and Rockwell, 1995; Magistrale, 1993; Ryan et al., 2009; Treiman, 1993) (Figure 1). Nevertheless, debate remains regarding the recent history of tectonic deformation (late Miocene to present) within the ICB; specifically, are active blind thrust systems responsible for the contractional folding and faulting observed in numerous seismic reflection datasets (Rivero et al., 2000), or are the compressional features observed within the ICB caused by restraining bends at stepovers along strike slip faults (Ryan et al., 2012)?

Reprocessed, industry multichannel seismic (MCS) reflection data were examined to characterize better the geometry of faulting in the ICB. Localized transpressional and transtensional deformation at fault bends and steps is observed, which is more consistent with a strike-slip style of deformation within the ICB. These fault discontinuities appear to control offshore deformation, which has implications for both seismic and tsunami hazard assessment. With the complex history of the ICB, which over the past ~20 m.y. has undergone extension, rotation, compression and translation, the improved continuity and resolution gained from reprocessed MCS data allows us to observe the interplay between modern and antecedent topography, sedimentation, and deformation.

Background

The ICB is a geomorphic region offshore southern California and Baja California, which has previously been characterized by a system of basins and ridges dissected by several dextral strike-slip fault zones (Figure 1) (Legg and Kennedy, 1979). Sedimentation in the ICB records the complex geologic history of the western margin of the North American plate in southern California (e.g., Bohannon and Geist, 1998; Crouch and Suppe, 1993; Legg, 1985; Nicholson et al., 1994). As subduction of the Farallon plate beneath western North America waned, the region underwent complex block rotation, extension, and transcurrent faulting associated with microplate capture and formation of the Transverse Ranges (Lonsdale, 1991, Nicholson et al., 1994, ten Brink et al., 2000). During this time (Oligocene to late Miocene?), the ICB experienced extensional and rotational deformation as a consequence of Pacific plate capture with rapid northwest motion relative to the North American plate. This deformation formed a vast system of basins and ridges that dominates the structure of the ICB. During the late Miocene, plate motion became more northerly (Atwater and Stock, 1998), the San Andreas transform system stepped landward into the Gulf of California-Salton Trough, and the deformation in the ICB decreased dramatically in magnitude and changed in style, becoming dominantly strike-slip.

Based on geodetic models, over 80 percent of the dextral motion between the Pacific and North American plates is accommodated by onshore faults (Becker et al., 2005; Bennett et al., 1996; Dixon et al., 2000; Meade and Hager, 2005) leaving between 10 and 20 percent (5-10 mm/yr) of the remaining slip budget to be distributed across active structures to the west and offshore. Such an estimate is consistent with long-term slip on the Agua Blanca fault (5-6 mm/yr, Figure 1) determined from trench sites (Rockwell, 2010).

The major fault zones previously mapped in the ICB south of Dana Point are the Newport Inglewood-Rose Canyon fault zone, Coronado Bank fault zone, San Diego Trough fault zone, Thirtymile Bank blind thrust, and Oceanside blind thrust (Figure 2A). Additionally, the San Mateo, San Onofre, and Carlsbad trends are zones of faulting and contractional folding mapped along the continental slope (after Rivero and Shaw, 2011) (Figure 2A).

The Newport Inglewood-Rose Canyon fault zone extends northwestward along the southern California coast from San Diego to West Los Angeles. South from Dana Point, the fault zone roughly follows the continental shelf edge to La Jolla Canyon, where it steps onshore north of Mount Soledad. The fault zone continues onshore

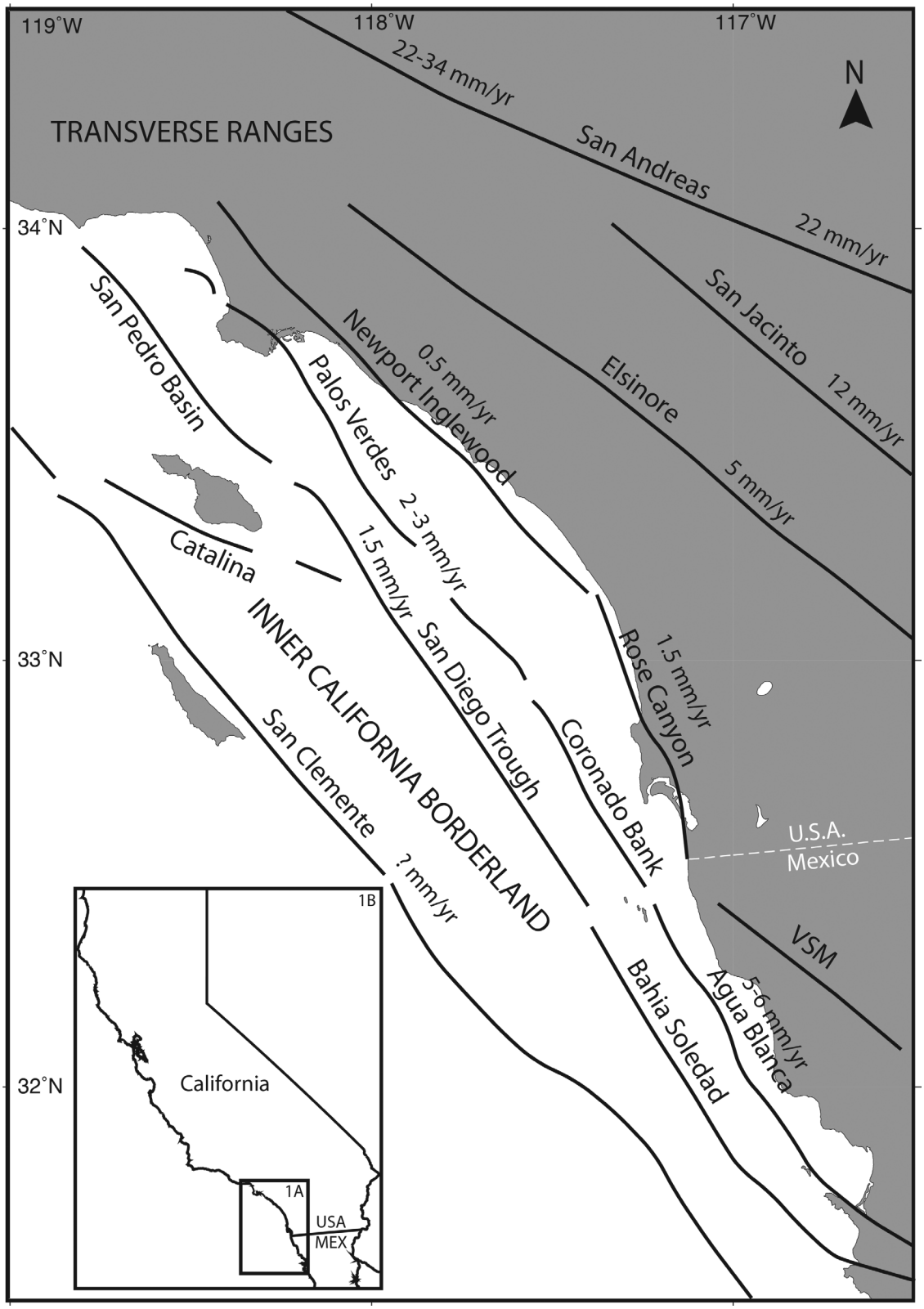

Figure 1. (A) Overview of the inner California borderland (ICB) region. Generalized fault traces and associated approximate slip rates are labeled. Slip rates are from Grant and Shearer (2004), with the exception of the San Diego Trough fault, which is from Ryan et al. (2012); VSM – Vallecitos – San Miguel fault. (B) Regional map of California with box illustrating the location of the inner California borderlands shown in Figure 1A.

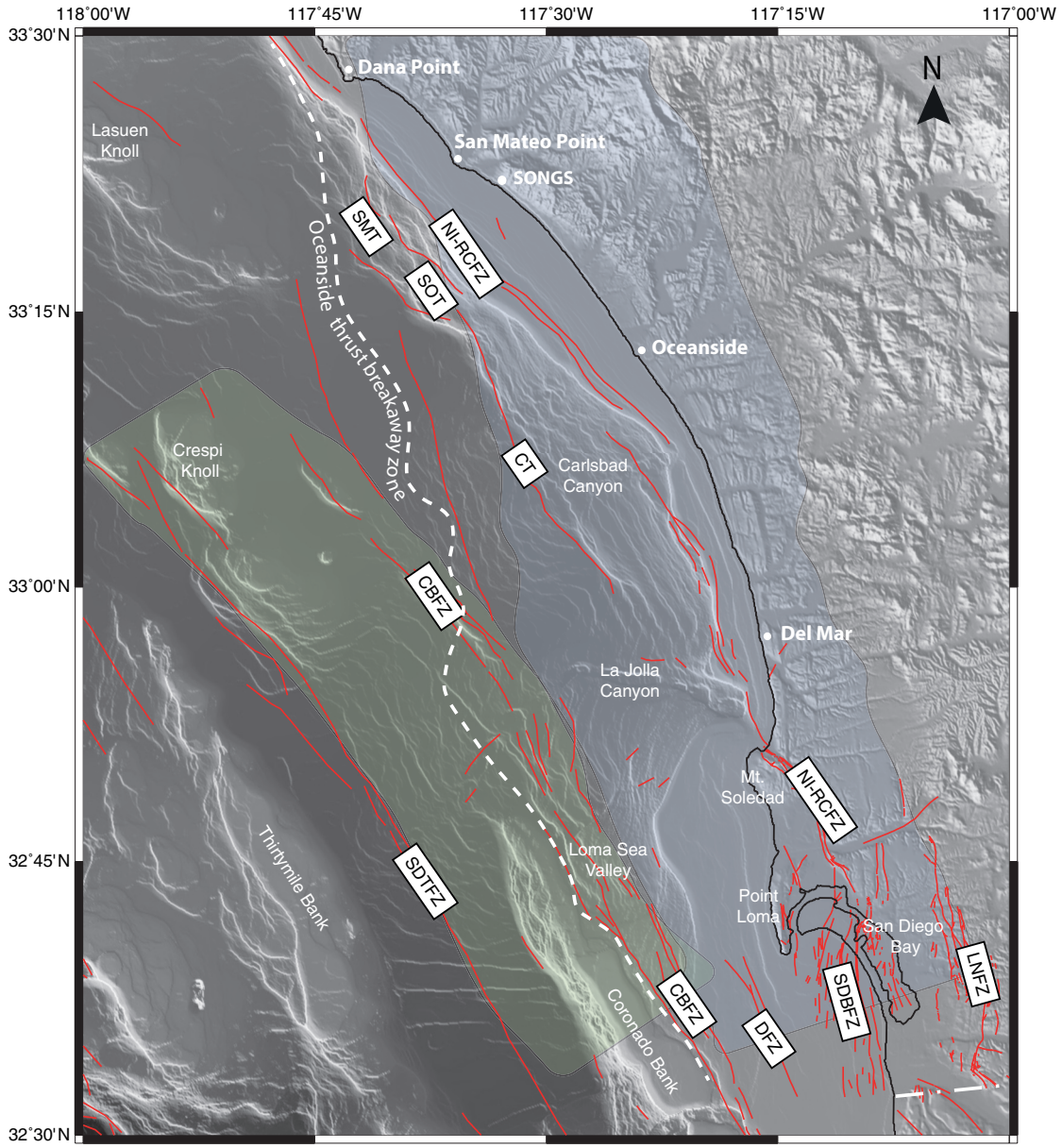

Figure 2a. (A) Shaded relief map of the inner California borderlands (ICB) highlighting major fault zones and purported thrust faults from Rivero and Shaw (2011). Major fault zones from the USGS database are shown in red and labeled: San Diego Trough fault zone (SDTFZ); Coronado Bank fault zone (CBFZ); Descanso fault zone (DFZ); La Nacion fault zone (LNFZ); Newport Inglewood-Rose Canyon fault zone (NI-RCFZ); San Mateo trend (SMT); San Onofre trend (SOT); Carlsbad trend (CT). Additionally, San Diego Bay faults are labeled as a group (SDBFZ) and include the Spanish Bight fault, Coronado fault, and Silver Strand fault. The fault surfaces mapped by Rivero and Shaw (2011) of the Thirtymile Bank blind thrust (green) and Oceanside blind thrust (blue) are shaded (depth of the fault surfaces are from z= 5 km to 17 km). The Oceanside thrust break away zone from Rivero and Shaw (2011) is shown by white dashed line and labeled.

along the I-5 corridor, and steps offshore again near downtown San Diego, where it splays into several faults within San Diego Bay. Offshore San Diego Bay to the south, the Newport Inglewood-Rose Canyon fault zone may step to the Descanso fault (Anderson et al., 1989; Kennedy and Welday, 1980; Legg, 1985), but may also be linked to the Vallecitos-San Miguel fault zone (Treiman, 1993; Wiegand, 1970). The Holocene slip rate on the Newport Inglewood-Rose Canyon fault zone was estimated to be ~1.5 mm/yr, determined from onshore trenching in San Diego (Lindvall and Rockwell, 1995; Rockwell, 2010). The post Miocene-Pliocene, long term slip rate along the northern, onshore portion of the Newport Inglewood-Rose Canyon fault zone was estimated to be ~0.5 mm/yr (Freeman et al., 1992).

The Coronado Bank fault trends ~N30°W and has been mapped from offshore Baja California to the La Jolla Fan valley. The fault zone varies in width and number of splays along strike (Kennedy and Tan, 2005; Legg, 1985; Ryan et al., 2009). Researchers have documented extensional structures along the Coronado Bank fault zone in Loma Sea Valley including conjugate normal faults, "monoclinal downwarping," and horst-graben structures, with some strands showing offset along the seafloor (Legg, 1985; Ryan et al., 2009). Nicholson (1994) and Sorlien et al. (1993) documented Miocene extension on the Coronado Bank fault as an east-dipping normal fault. Rivero et al. (2000) suggested that the Coronado Bank fault was reactivated as the Oceanside blind thrust fault from Dana Point to the US-Mexico border. In regional models, the Coronado Bank fault is assumed to transfer slip to the Palos Verdes fault zone to the north, but recent evidence suggests that the two may not be connected (Ryan et al., 2012) and slip-rates on the Coronado Bank fault have not been directly measured.

Approximately 30 km offshore San Diego, the San Diego Trough fault trends ~N30°W through the San Diego Trough submarine basin. Through the basin, the fault zone is mapped as a relatively straight and simple fault trace (Legg, 1991), but bends and steps have been mapped near Crespi Knoll and Santa Catalina Island (Ryan et al., 2012). To the south, the San Diego Trough fault joins with the Bahia Soledad fault offshore northern Baja California (Legg, 1991), while to the north the fault zone may be linked with the San Pedro basin fault zone (Ryan et al., 2009; Ryan et al., 2012). The slip rate on the San Diego Trough fault was estimated to be ~1.5 mm/yr through the Holocene (Ryan et al., 2012).

Recent studies purport that extensional, low angle detachment surfaces have been reactivated as blind thrust faults in the ICB (Rivero and Shaw, 2011; Rivero et al., 2000), and locally influence the distribution of tectonic strain between low-angle faults and high angle lateral faults. The Oceanside blind thrust, Thirtymile Bank blind thrust, and associated deformation, have been mapped with legacy industry seismic reflection profiles extending from Dana Point to the US-Mexico border (Figure 2A) (Rivero and Shaw, 2011). Rivero and Shaw (2011) and Rivero et al. (2000) interpret vertical faults to merge with, or be offset by the low-angle blind thrust surfaces. The Thirtymile Bank blind thrust has been identified to explain the location of seismicity associated with the 1986 Oceanside earthquake (Astiz and Shearer, 2000), as well as a partial thrust component of the main shock (Rivero and Shaw, 2011).

The San Mateo trend, San Onfore trend, and Carlsbad trend are contractional structures (anticlines and faulted anticlines) that have been attributed to the Oceanside blind thrust (Rivero and Shaw, 2011), or alternatively to localized contraction associated with strike-slip faulting on the Newport Inglewood-Rose Canyon fault zone (Crouch and Bachman, 1989; Fisher and Mills, 1991). The San Mateo and San Onofre trends are mapped west of the Newport-Inglewood-Rose Canyon fault zone, offshore from San Onofre, whereas the Carlsbad trend extends farther south and terminates offshore north of Del Mar (Figure 2A). Rivero and Shaw (2011) observed these trends soling into the Oceanside blind thrust at depth and interpreted the structures as forethrusts. These trends have been identified as active structures that produce topography on the seafloor (Rivero and Shaw, 2011).

An alternative to the blind thrust model has strike-slip faults controlling the Quaternary tectonics of

the ICB, with compressional and extensional components formed by bends and steps in offshore strike-slip fault zones (Newport Inglewood-Rose Canyon fault zone, Coronado Bank fault zone, San Diego Trough fault zone). Ryan et al. (2012) suggest that the 1986 Oceanside earthquake was located in an area of transpression associated with a restraining bend in the right-lateral, strike-slip San Diego Trough fault. Additionally, Ryan et al. (2009) put forth an alternative explanation for the observed compressional deformation associated with the Oceanside blind thrust that involves a clockwise rotating block between the Coronado Bank fault zone and Newport Inglewood-Rose Canyon fault zone. They reported areas of both extension and compression in seismic data from the ICB and therefore propose that deformation is explained better by rotation associated with large strike-slip faults versus regional thrust systems.

Methods

This study examined reprocessed industry MCS profiles from Chevron geophysical surveys (Figure 2B). We acquired original SEG-Y field records from the 1979 Chevron MCS datasets (H-17-79 and H-18-79). Approximately 950 line-km of the 1979 Chevron data along 29 seismic profiles were reprocessed. Some MCS lines in the USGS archive were concatenated onto other lines, which required some level of profile reconstruction. The direct arrival was used to assign source-receiver offset, as this critical information was not available. Original geometry included a 96 channel hydrophone streamer, with 110 foot spacing of receivers, coincidently matched by a 110 foot shot spacing interval; this provided 48 fold data in common midpoint space (55 foot separation). Reprocessing was conducted in cooperation with Geotrace, and included a hybrid multiple suppression scheme (e.g., SRME), trace interpolation in shot and receiver space, and prestack time migration (PSTM). The coarse receiver spacing limits some modern processing approaches for prestack migration, and demultiple approaches due to issues with spatial aliasing; however, the processing scheme leveraging trace interpolation greatly improved the surficial resolution and continuity of reflectors down to ~2.5 seconds Two-Way Travel Time (TWTT) and removed the seafloor multiple. We employed a sequence stratigraphic approach to establish a chronostratigraphic framework and define the relative timing of deformation (Christie-Blick and Driscoll, 1995).

Results

Newly reprocessed industry MCS data are presented from north to south in the region offshore between San Onofre and Del Mar (Figure 2B). To clarify interpretation of the San Mateo, San Onofre, and Carlsbad trends (modified after Rivero and Shaw, 2011), we employ the following nomenclature based on the strike of the faults and the observed deformation and dip of the seafloor west of the trends. Where the faults are northwest trending and the stratigraphy and seafloor dip to the west, we refer to the structure as the San Mateo trend. The San Onofre trend is where the stratigraphy and seafloor to the west are flat-lying, but the fault zone maintains a similar strike to the San Mateo trend (Figure 2A). Finally, the Carlsbad trend is where the strike of the fault becomes more northerly, with the stratigraphy and seafloor remaining relatively flat lying to slightly eastward dipping.

MCS line 4516 (Figure 3), a dip line located offshore of San Mateo Point (Figure 2B), reveals a high-amplitude, low-frequency basal reflector, which is inferred to represent acoustic basement (Figure 3, blue horizon). The acoustic basement shoals from 2+ seconds TWTT in the east towards the west, where it crops out/subcrops along the southern extent of Lasuen Knoll (Figure 2B). Basement in this region of the ICB is predominately composed of the Catalina Schist (Bohannon and Geist, 1998). The acoustic basement reflector is offset and fragmented by a series of high angle faults. Toward the center of the basin (near shot 350) the high angle faults are associated with a deformational ridge that offsets the blue horizon and deforms both the red and green horizons (a positive flower structure). The onset of deformation in this region is difficult to identify with confidence based on stratal geometry; however, deformation and rotation of the stratal packages above the dashed red horizon are observed (Figure 3). The

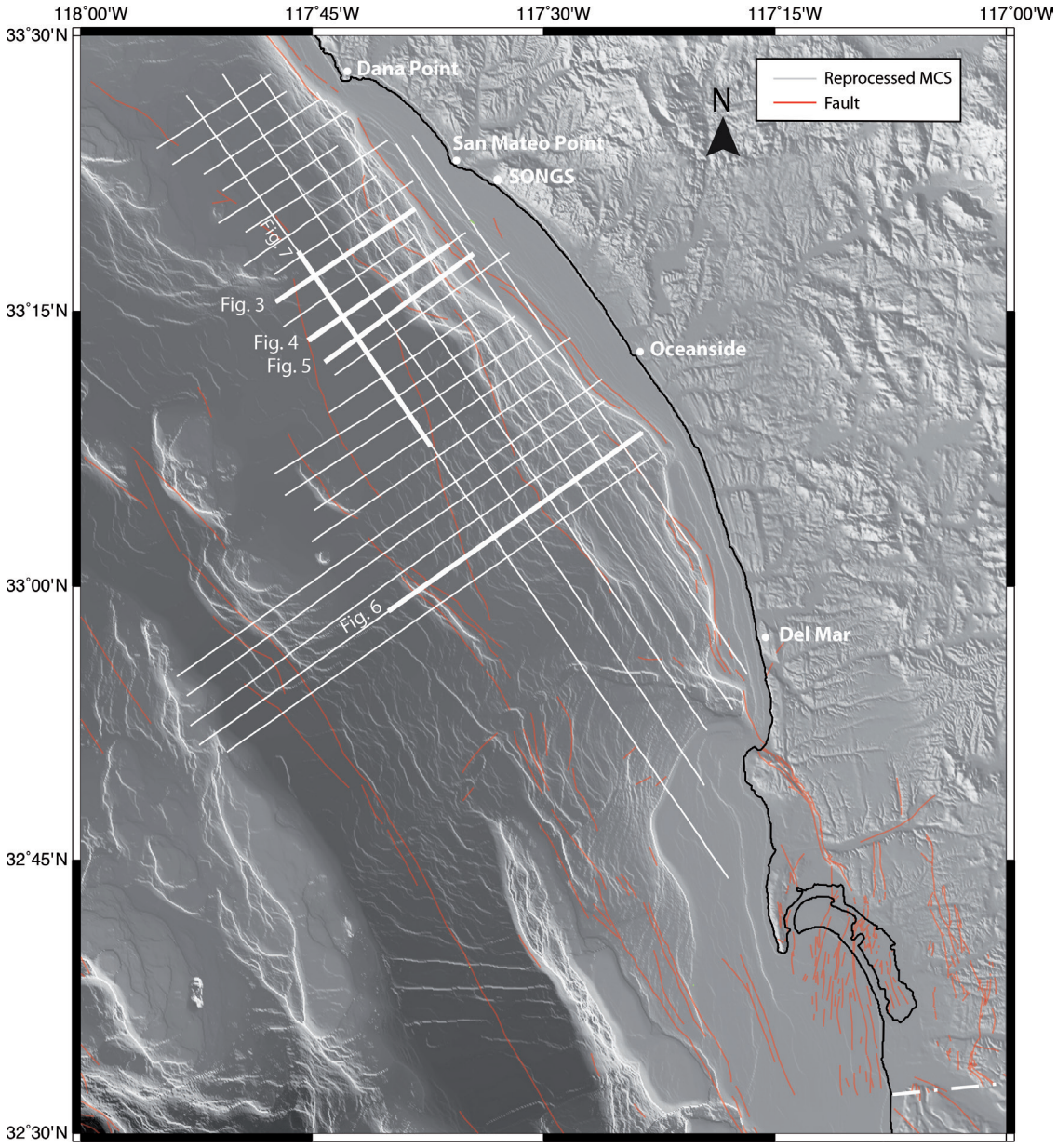

Figure 2b. (B) Shaded relief map showing location of reprocessed MCS data used in this study (white). Faults from the USGS database are shown in red.

basin strata have a westward dip that diminishes up section. On the east end of Figure 3, the San Mateo trend delineates a change in slope and appears to offset the seafloor. Furthermore, the faulted and offset acoustic basement can be observed to the east and appears offset by the San Mateo trend.

Continuing south, MCS line 4520 (Figure 4a) is offshore, slightly south from the San Onofre Nuclear Generating Station (SONGS; Figure 2B). The acoustic basement in this region exhibits less relief than farther north (e.g., Figure 3) and is best imaged in the seismic data west of the San Onofre trend. The sediment package below the red horizon and above acoustic basement is well laminated and roughly concordant (Figure 4a). Based on correlation with industry wells (Mobil MSCH-1 San Clemente Well after Rivero and Shaw, 2011), these packages are middle Miocene to Pliocene

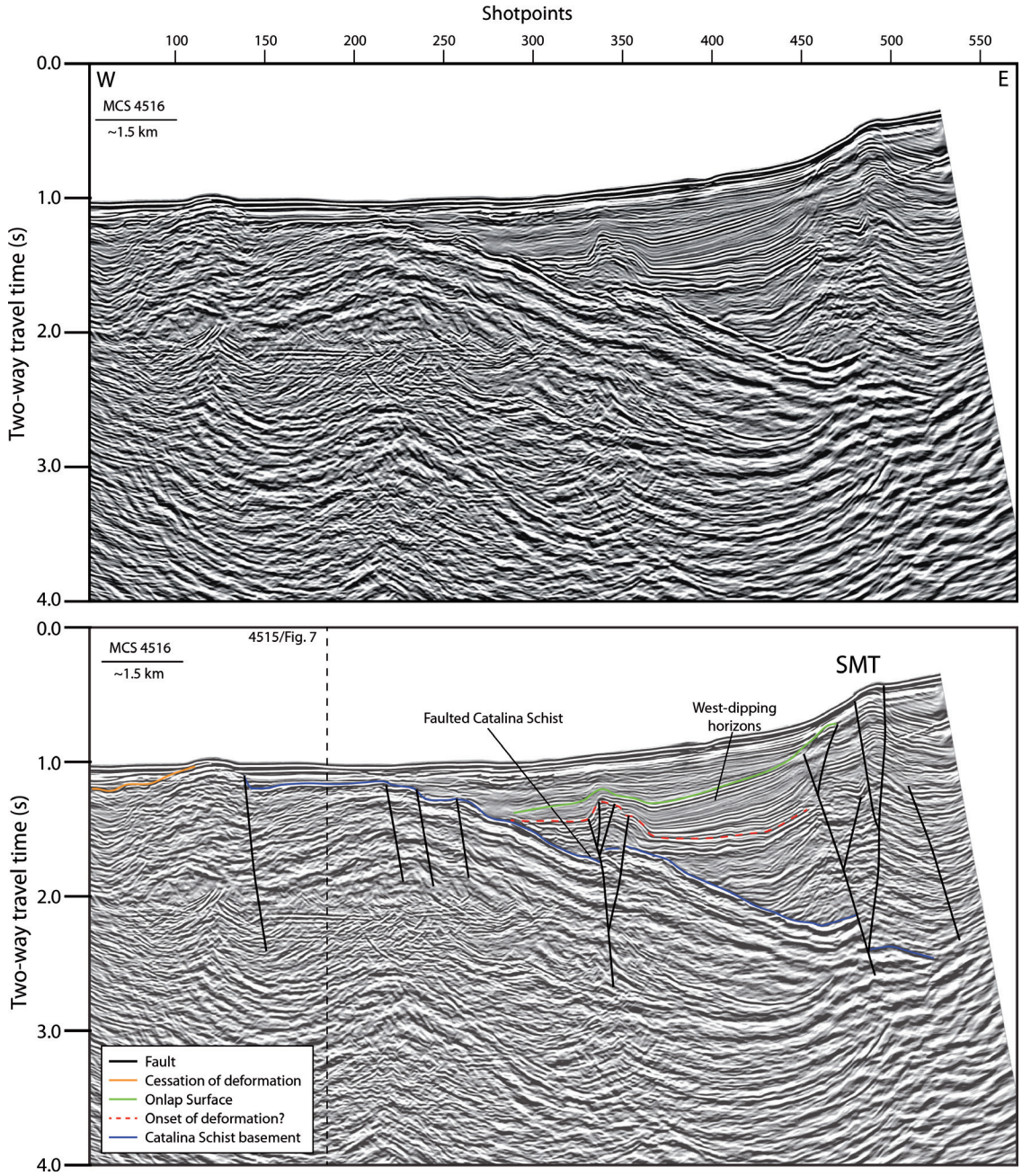

Figure 3. Un-interpreted (top) and interpreted (bottom), re-processed MCS line 4516 illustrating deformation west of the San Mateo trend. Horizons regionally dip to the west and onlap the acoustic basement, which is fragmented and offset by several faults. A faulted structure offsets the basement near shot 350. Profile location is shown in Figure 2B. See inset legend for interpretation key. Vertical dashed line shows intersection with labeled profile 4515. Abbreviation: SMT – San Mateo trend.

deposits including from oldest to youngest, the San Onofre Breccia, Monterey Formation, San Mateo Formation, Capistrano Formation, Repetto Formation, and lower Pico Formation (Sorlien et al., 2009; Rivero and Shaw, 2011). Nevertheless, limited well data and faulting along the margin make exact correlations difficult. Therefore, we employ only relative timing of deformation and style along the margin. A tilted block is imaged along the western portion of the profile above acoustic basement, with well-imaged internal laminations (Figure 4a). The reflectors within the block terminate against

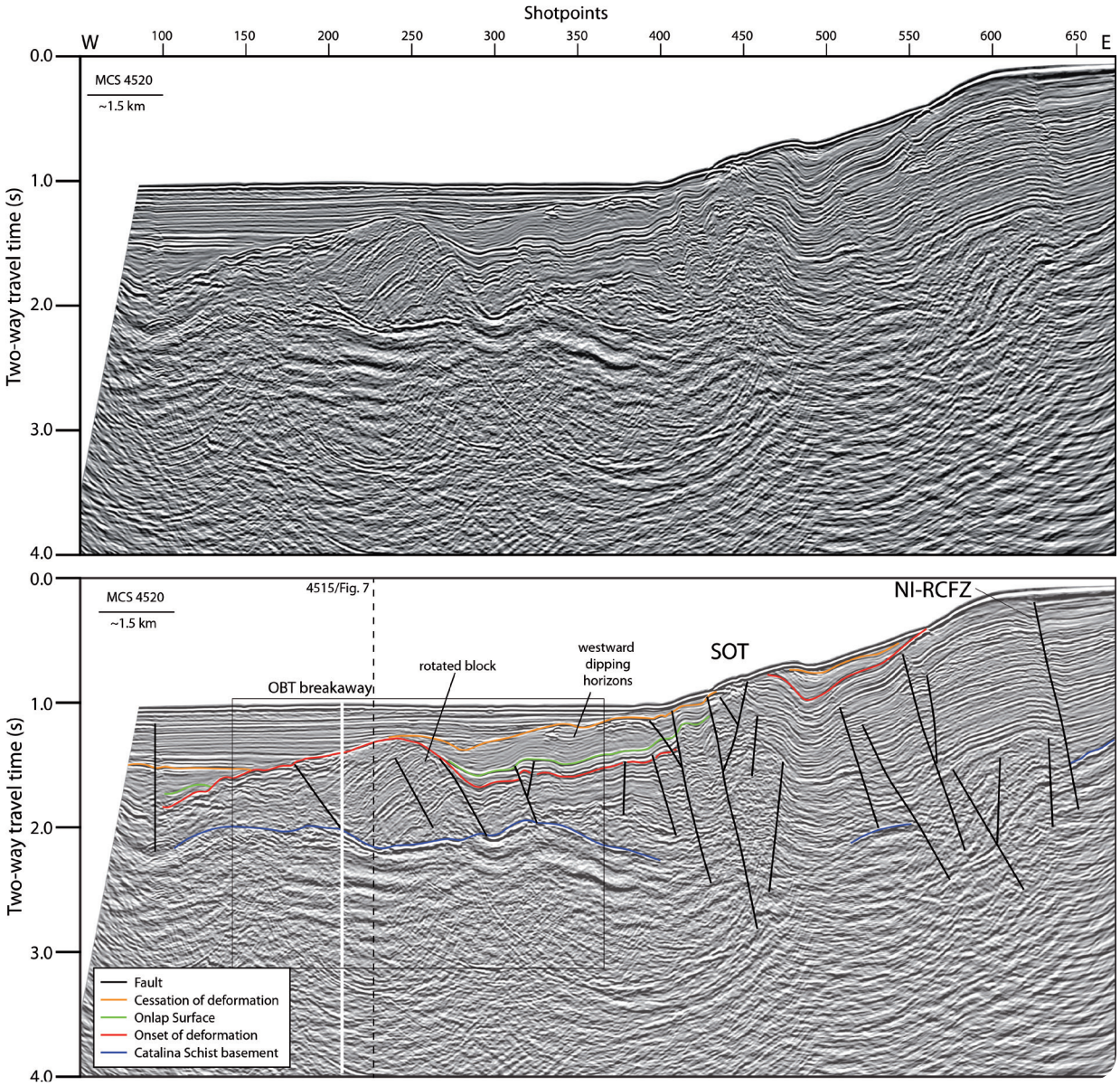

Figure 4a. Un-interpreted (top) and interpreted (bottom), re-processed MCS line 4520 imaging deformation at the San Onofre trend and Newport Inglewood-Rose Canyon fault zone. Horizons west of the San Onofre trend above the orange horizon are regionally flat-lying and locally dip slightly to the west. The vertical white line marks the geographic location of the Oceanside blind thrust breakaway zone mapped in Rivero and Shaw (2011). Profile location is shown in Figure 2B. See inset legend for interpretation key. Vertical dashed line shows intersection with labeled profile. Abbreviations: SOT – San Onofre trend; NI-RCFZ – Newport Inglewood-Rose Canyon fault zone; OBT – Oceanside blind thrust.

the acoustic basement (Figure 4b). The acoustic character of the tilted block is similar to reflectors imaged on the upper slope and outer shelf (e.g., shotpoints 550-650). Above the red and green horizons, the sediment packages onlap structural highs, and are rotated and deformed; the packages have an overall westward dip. Continuing upsection, the orange horizon separates rotated and deformed sediment below from flat lying, undeformed sediment above (Figures 4 and 4b). West of the San Onofre trend, the faults are inactive and do not offset the orange reflector, and most faults do not offset the red reflector. Moving east near the San Onofre trend, the reflectors are folded (anticline-syncline

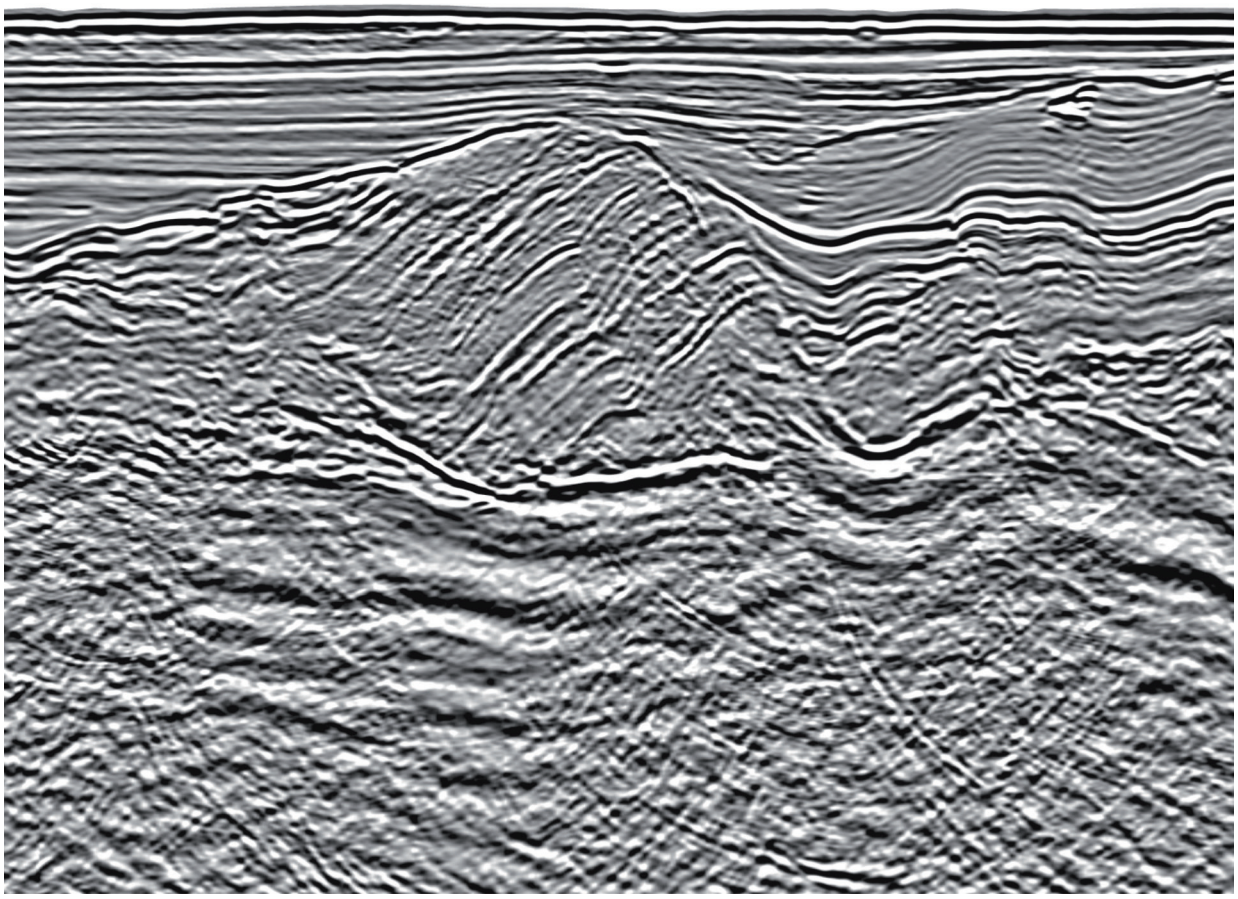

Figure 4b. Enlarged section of MCS line 4520 shows the relationship between the rotated block and the underlying acoustic basement. The reflectors terminate against the acoustic basement. Flat lying reflectors onlap the western portion of the rotated block. Box in Figure 4a shows the location of the enlarged profile.

pair), faulted and uplifted, with east side up over west. The amount of folding across the San Onofre trend in Figure 4a appears slightly greater than that observed across the San Mateo trend in MCS line 4516 (Figure 3). East of the San Onofre trend, there are a series of eastward dipping faults that may be splays of the San Onofre trend and Newport Inglewood-Rose Canyon fault zone, which are observed along the eastern margin (Figure 4a).

Farther south, MCS line 4522 (Figure 5a), which is similar to line 4520, reveals a systematic pattern of deformation that progressively gets younger toward the east. Younger stratigraphic horizons toward the east are deformed. For example in Figure 5a, above the relatively flat-lying acoustic basement, the tilted block with well-imaged acoustic laminations is onlapped by flat-lying sediments above the green horizon and below the orange horizon. Farther east, fault structures offset and deform the green and orange horizon (Figures 5 and 5b). Nevertheless, faults west of the San Onofre trend are dormant as the orange horizon is onlapped by flat-lying reflectors that show no signs of deformation. The stratigraphic packages bounded by the red and orange horizons are predominantly flat-lying with no regional dip. Near the San Onofre trend, the deformation appears more distributed with less folding than observed on line 4520 (Figure 4a); horizons very close to the seafloor appear offset (Figure 5a). In this region, the dip of the Newport Inglewood-Rose Canyon fault zone appears slightly steeper

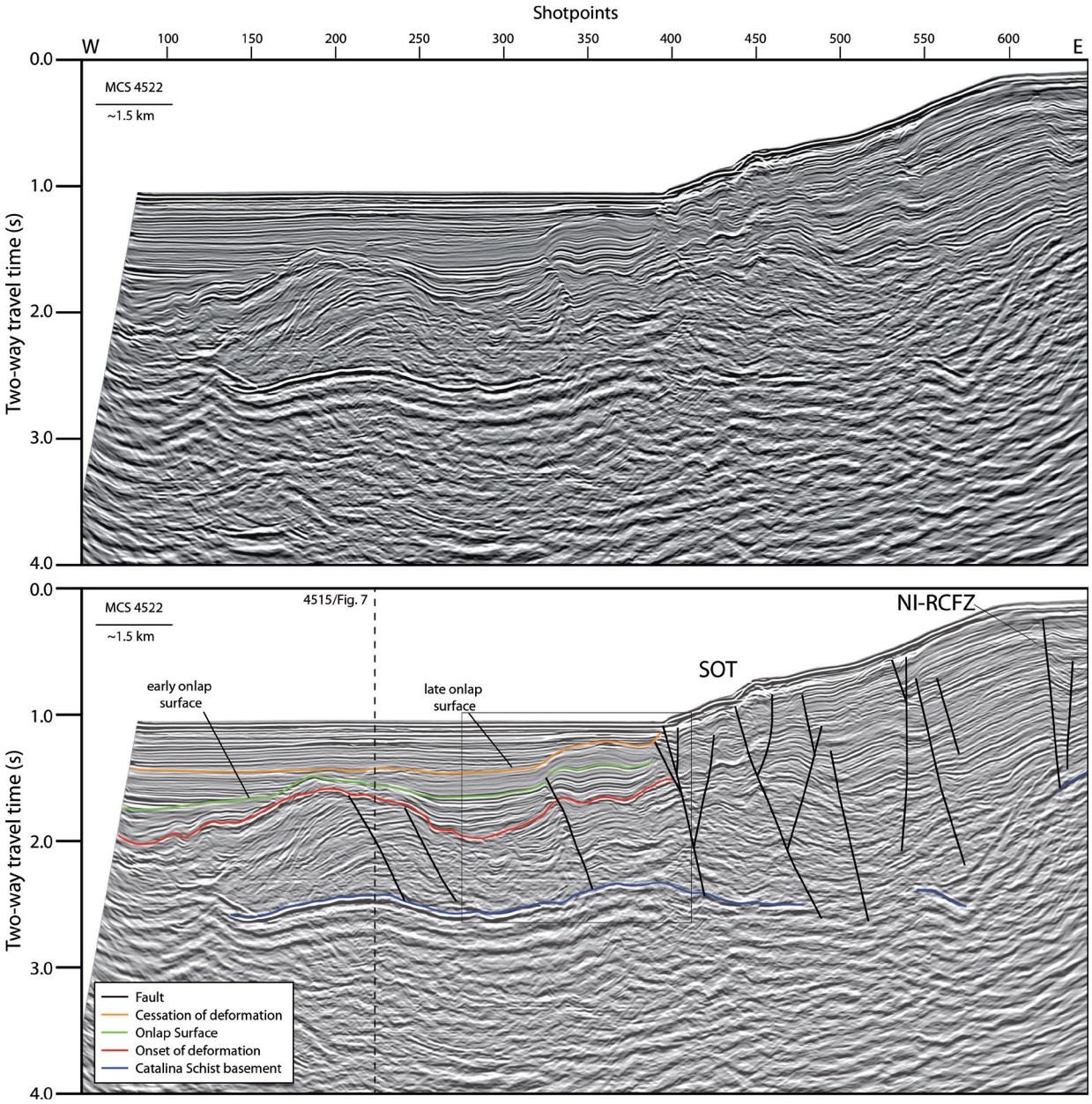

Figure 5a. Un-interpreted (top) and interpreted (bottom), re-processed MCS line 4522 illustrating deformation at the San Onofre trend and Newport Inglewood-Rose Canyon fault zone. Horizons west of the San Onofre trend above the red horizon are relatively flat lying. Note the reflectors above the green horizon are flat lying and undeformed in the west, whereas toward the east the reflectors above the green horizon are folded and deformed, as observed from the early and late onlapping surfaces annotated on the interpreted profile. Profile location is shown in Figure 2B. See inset legend for interpretation key. Vertical dashed line shows intersection with labeled profile. Abbreviations: SOT – San Onofre trend; NI-RCFZ – Newport Inglewood-Rose Canyon fault zone.

than to the north and we interpret the blue reflector (acoustic basement) to be offset up to the east along the fault zone.

The Carlsbad trend is a narrow fault zone that exhibits two strikes. North of the Carlsbad Canyon, the trend is more northerly compared to the San Mateo and San Onofre trends (Figure 2). Seaward, there are two additional faults (an unnamed fault and a splay of the Coronado Bank fault) that exhibit a similar trend roughly parallel to the Carlsbad trend north of the Carlsbad Canyon (Figure 2). South of Carlsbad Canyon, the Carlsbad trend is

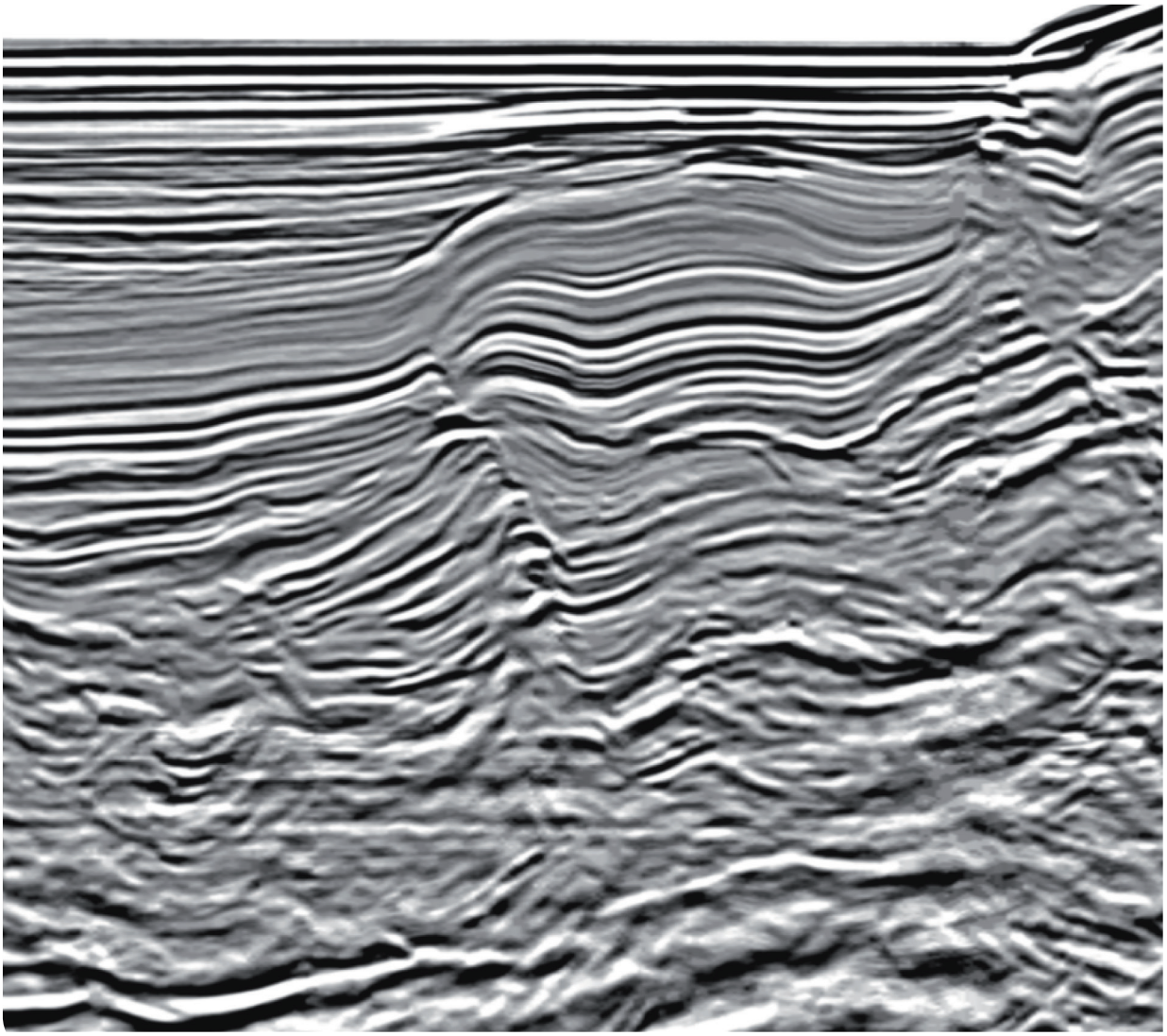

Figure 5b. Enlarged section of MCS line 4522 shows the fault fold structure along the base of the slope. Flat lying reflectors onlap the fault fold structure and the deformation is younger toward the east. Box in Figure 5a shows the location of the enlarged profile.

more northwest, which is more parallel to the San Mateo and San Onofre trends (Figure 2a). These changes in strike along the Carlsbad trend and the consequent styles of deformation are observed in the reprocessed MCS data. For example in MCS line 4542 (Figure 6), west of the Carlsbad trend, the stratigraphic packages bounded by the red and orange horizon dip to the east with the dip increasing down section. The faults west of the Carlsbad trend and east of the Coronado Bank fault zone appear to have a normal dip-slip component and do not offset the orange reflector (Figure 6). Flat-lying reflectors above the orange horizon onlap onto the deformation associated with the Carlsbad trend and, more importantly, mantle the Carlsbad trend. The deformation associated with the Carlsbad trend has little to no bathymetric expression in this region (Figure 6). The deformation in this region where the Carlsbad trend has a more northwest trend (Figure 2b) appears transpressional with the green and orange horizon being up on the east side of the fault (Figure 6). East of the Carslbad trend, the reflectors above acoustic basement dip to the west with slight westward thickening. A strand of the Newport Inglewood-Rose Canyon fault zone is imaged farther up slope and dips to the west. The basement high toward the west in line 4542 aligns with Coronado Bank farther to the south and

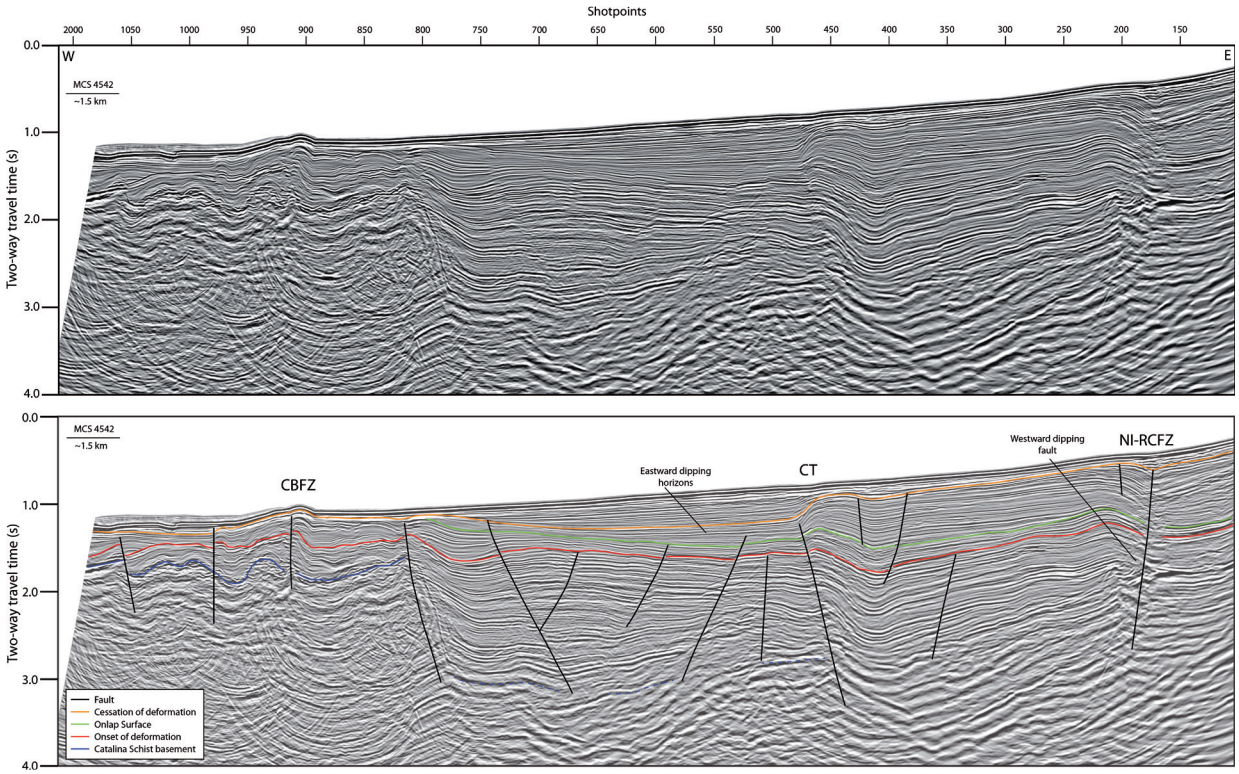

Figure 6. Un-interpreted (top) and interpreted (bottom), re-processed MCS line 4542 illustrating transtensional deformation west of the Carlsbad trend. Note reflectors bounded by the red and orange horizons west of the Carlsbad trend diverge and dip towards the east. Onlapping reflectors mantle the deformation associated with the Carlsbad trend. Profile location shown in Figure 2B. See inset legend for interpretation key. Abbreviations: CT – Carlsbad trend; NI-RCFZ – Newport Inglewood-Rose Canyon fault zone.

faulting in that area appears associated with the Coronado Bank fault zone (Figure 2).

Based on observations from this series of MCS dip lines, an important demarcation exists between the San Mateo and the San Onofre and Carlsbad trends. Deformation appears more recent from the San Mateo trend to the north (Figure 3), whereas there is no recent deformation observed west of the San Onofre and Carlsbad trends (Figures 5 and 6). In addition, the different trends are associated with different deformation styles (Figure 2A).

MCS line 4515 (Figure 7a) is a strike line that trends parallel to the margin and crosses the western portion of MCS lines 4516, 4520, and 4522 (Figure 2B). Toward the north, the acoustic basement has a diagnostic high amplitude reflector with a low-frequency acoustic character and crops out/subcrops in the vicinity of southern Lasuen Knoll (Figure 2), offshore Dana Point (Figures 3 and 7). Moving south, the acoustic basement exhibits a pronounced change in slope (ramp) between the flat-lying basement to the north and the gently dipping regional basement to the south. There is approximately 2.5 seconds TWTT of relief on the acoustic basement with the greatest depths observed offshore La Jolla (Figure 2B). The reflectors between the acoustic basement and red horizon dip north with an increase in dip with depth (Figures 7 and 7b); adjacent to the basement, these reflectors exhibit a slight reversal of dip, creating an asymmetric syncline where the basement slope changes. In east-west profiles (e.g., 4520 and 4522) across this deformed structure, faulted strata within the block dip to the west (Figures 4 and 5). Moving south along the acoustic basement interface (down section) there appears to be an increase in deformation and acoustic imaging becomes limited (Figure 7b). Structures and deformed strata are observed in the overlying carapace that might be indicative of fluid expulsion (Figure 7a). The onlapping packages above the red and green horizon show evidence of

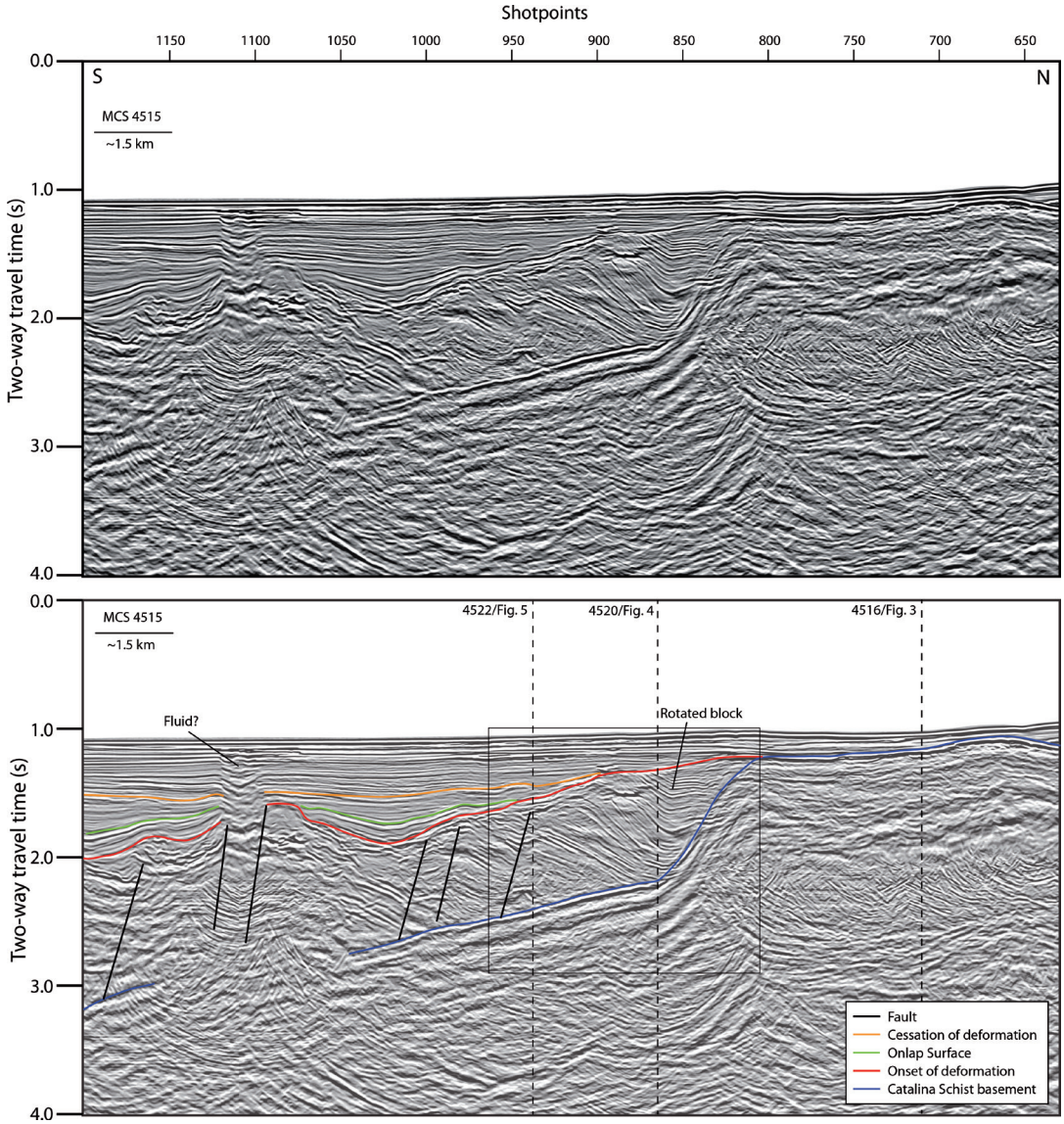

Figure 7a. Un-interpreted (top) and interpreted (bottom), re-processed MCS line 4515 illustrating acoustic basement relief and the rotated and deformed reflectors. The dip of the reflectors increases with depth and the minor reversal in dip may represent small drag folds. Note that deformation increases down-section and reflector clarity diminishes. The basement dips to the south, away from the high in the north (offshore Dana Point). Lens shaped reflections in the overlying carapace between shots 1100-1150 may be recording fluid expulsion. Profile location is shown in Figure 2B. See inset legend for interpretation key. Vertical dashed lines show intersection with labeled profiles.

minor deformation, with no deformation observed in the flat-lying packages above the orange reflector.

Discussion

Controversy remains regarding the origin of the observed late Pliocene to present deformational features in the ICB. Rivero et al. (2000) proposed the explanation that much of the compressional deformation observed along the margin was caused by the reactivation of extensional detachments, including the Oceanside blind thrust and Thirtymile Bank blind thrust. In 2000, this new idea gained much traction in light of the recent Northridge thrust earthquake (1994). Conversely, other models in the ICB propose that the deformational patterns are caused by a combination of compressional and extensional jogs in the dextral fault systems offshore, and/or by large block rotation (Ryan et al., 2012; 2009).

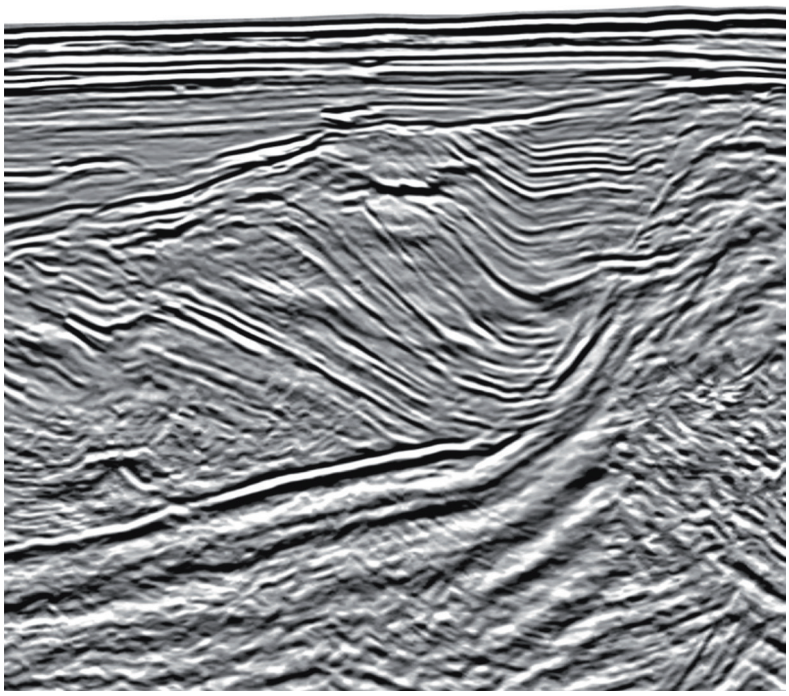

Figure 7b. Enlarged section of MCS line 4515 shows the rotated block with dips increasing down-section. Flat lying reflectors onlap the fault fold structure and the deformation is younger toward the east. Box in Figure 7a shows the location of the enlarged profile.

Rivero et al. (2000) and Rivero and Shaw (2011) presented several lines of evidence to support their hypothesis regarding the Oceanside blind thrust. First and foremost, faults and folds in the overlying carapace do not offset the Oceanside blind thrust. The second is an outgrowth of the first, and states that the Oceanside blind thrust can be continuously mapped along the margin and that more vertical faults merge into the Oceanside blind thrust at depth. Finally, their structural cross-sections balanced, lending support to their interpretation, which suggested approximately 2 – 2.4 km of shortening. Age constraints on the timing of this deformation are poor; however, if the Oceanside blind thrust became active in the late Pliocene, then based on Rivero and Shaw's (2011) reconstructions the contraction rate is approximately 0.5 - 1.5 mm/yr with an attendant uplift rate of approximately 0.27 – 0.40 mm/yr.

The Oceanside blind thrust is interpreted to reactivate normal faults (Rivero and Shaw, 2011; fig. 6). Based on industry MCS data, Rivero and Shaw (2011) map the Oceanside detachment from the surface breakaway zone to depths of >6 km (Rivero and Shaw, 2011; fig. 2). The detachment surface has a northwest strike with a uniform northeast dip. It is difficult to map the inferred detachment to the east in the seismic data; nevertheless, Rivero and Shaw (2011) project a plane from the base of the mapped surface at 5 km, which is roughly coincident or slightly east of the San Mateo and San Onofre trend, and west of the Carlsbad trend (Figure 2a), to a depth of 17 km (Rivero and Shaw, 2011; fig. 6). This plane is the purported seismogenic zone for the Oceanside blind thrust (Figure 2a). The new reprocessed MCS data reveal that the deformation along the Oceanside thrust breakaway zone is inactive as it is onlapped by late Pliocene flat-lying strata (Figure 4a). Furthermore, deformation west of the San Mateo, San Onofre, and Carlsbad trends also is dormant at least since the orange horizon (Figures 4, 5, and 6). Onlapping turbidites reveal that the deformation becomes younger towards the east; an observation not consistent with a westward verging blind thrust fault system – such as the Oceanside blind thrust. Finally, the new data show that the inferred Oceanside detachment is most likely the top of the Catalina Schist and cannot be

confidently mapped toward the east under the continental shelf (Figures 4, 5, and 6). In summary, the reprocessed MCS data improved reflector continuity and resolution that provided important new constraints on ICB tectonic deformation and margin architecture. A sequence stratigraphic process-oriented approach was employed to interpret the reprocessed MCS data (Christie-Blick and Driscoll, 1995), which places important constraints on the relative timing of deformation across and along the margin. We will first discuss the character of the acoustic basement, then focus on the deformation above the acoustic basement and finally on the timing of deformation across the margin.

In MCS line 4516, the acoustic basement is fragmented and offset by many fault zones (Figure 3). The positive flower structure observed in the basin is more consistent with steep vertical faults than a low-angle thrust. Along MCS lines 4520 and 4522 (Figures 4 and 5), the acoustic basement exhibits much rugosity, and west of the San Onofre trend is roughly horizontal, with little to no fault offsets observed. On all of the reprocessed lines it is difficult to trace the acoustic basement (inferred Oceanside blind thrust) landward beyond the San Mateo, San Onofre, and Carlsbad trends (Figures 4, 5, and 6). One might argue that in the other legacy MCS data, or in depth sections, the Oceanside blind thrust appears more continuous and can be traced laterally farther to the east under the margin (e.g., Rivero and Shaw, 2011). The main problem with the legacy data is that during stacking, some wide-angle reflection/refraction (i.e., caustics) were misinterpreted as near normal incidence reflections and improperly stacked; this gave the reflectors their high amplitude and low frequency character. This approach provided greater apparent continuity to the Oceanside blind thrust reflections, which is not observed in the new PSTM imagery. For clarity, we distinguish the detachment from the thrust in the following ways: (1) the detachment surface accommodated Miocene extension along the margin during the reorganization (Bohannon and Geist, 1998), and (2) the thrust is where the detachment has been reactivated in compression. It is important to note that the detachment has a complicated geometry and may comprise both an east- and west-dipping component (Bohannon and Geist, 1998; ten Brink et al., 2000). In our interpretation, the high amplitude reflectors with a low frequency acoustic character are more indicative of a basement surface than an active fault surface (Figures 3 and 4). The largest relief on the basement is toward the south, parallel to the margin; acoustic basement is >2.5 seconds TWTT offshore of La Jolla (southern end of Figure 7a). This deep basin corresponds to a gravity low (Smith and Sandwell, 1997). The basin fill is offset by the un-named faults that have a more northerly trend than the other main fault zones and may be accommodating transtension across a releasing step between the Coronado Bank fault and Newport Inglewood fault. This step-over may also explain the dying away of the Coronado Bank fault to the north. The deformed block above acoustic basement is observed in Figure 7a and the rotated strata and possible drag folding indicate transport towards the south-southeast, into the basin and gravity low, as illustrated in the fence diagrams shown in Figures 8 and 9. MCS Line 4515 is roughly sub-parallel to the trend of the proposed Oceanside blind thrust (Rivero and Shaw, 2011). In their model, the predicted transport direction or vergence of the hangingwall is to the southwest. In contrast, the fence diagrams show that that the transport direction of the tilted and deformed block is to the south-southeast (Figures 8 and 9). The basement depth systematically increases toward the south from near the seafloor at Lasuen Knoll to >2.5 km offshore La Jolla. In addition, the thickness of the onlapping fan sequences also increases to the south east of the Coronado Bank fault.The basin most likely has a composite history recording both Miocene extensional deformation and late Miocene to present transtensional deformation. The onlapping strata indicate that rotation and deformation of the block have not occurred since the green sequence horizon (Figures 4, 5, and 7). In summary, the fragmentation, geometry, and north-south relief on the acoustic basement, and south to southeast block transport imaged in the reprocessed data are more consistent with strike-slip deformation superposed on Miocene extensional structures (Figure 10) than a regional thrust system. Our observations of the south to south-east transported deformed block, and minimal deformation since the green horizon (Figures 8 and 9), are also

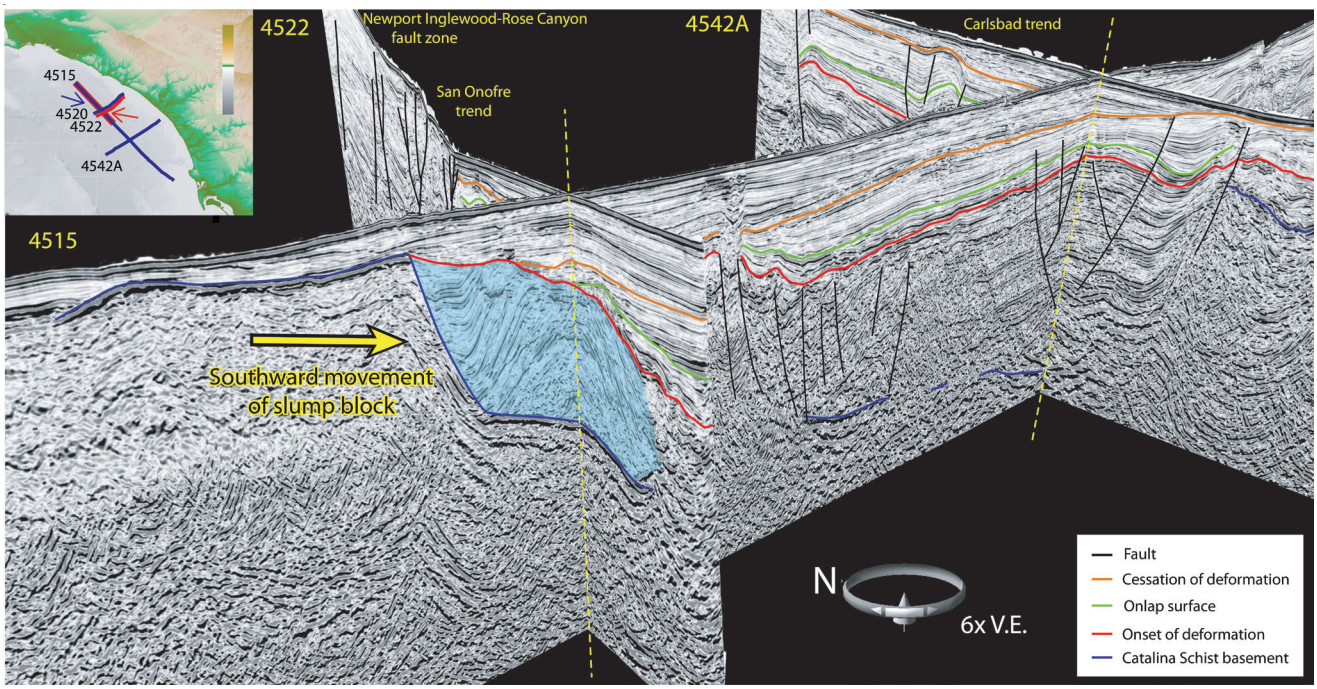

Figure 8. Fence diagram showing the reprocessed and interpreted MCS lines in a three dimensional perspective. The dashed yellow line marks the intersection between the profiles, and the shaded blue area denotes the approximate extent of the rotated block. The inset map is color-coded to show the perspective (arrows) and lines displayed in each diagram: blue lines for Figure 8; red lines for Figure 9. Lines 4515, 4522, and 4542A viewed for the northwest shows the southward transport direction of the rotated block.

inconsistent with a large block rotation model as proposed by Ryan et al. (2009).

We observe several changes in deformational patterns moving from north to south through the central ICB region. West of the San Mateo, San Onfore, and Carlsbad trends, we observe a change from compressional deformation in the north to extensional deformation and divergence in the south (Figures 3, 4, 5 and 6). In concert, the dip of the stratigraphic units bounded by the red and orange horizons changes from west dipping offshore the San Mateo trend, to flat-lying west of the San Onofre trend, to east dipping west of the southern Carlsbad trend. These observations of both transtension and transpression are difficult to explain by a regional thrust system, such as that proposed by Rivero et al. (2000) and later by Rivero and Shaw (2011).

In the region of the ICB studied here, the character of faulting varies along strike of major fault zones (Figure 2A). Evidence from seismic data indicates that some of this variability is caused by transtensional and transpressional jogs along dextral fault systems as well as changes in trend from a more northerly strike to a northwest strike. In the central ICB, the area defined in Figure 6 west of the Carlsbad trend appears to be a zone of extension created by a right step from the Coronado Bank fault zone to the Newport Inglewood-Rose Canyon fault zone; deformation in this relay zone is now inactive. The step-over zone offsets onlapping sedimentary packages infilling deep basins with associated gravity lows (Smith and Sandwell, 1997). Given the orientation of faults in this area of the ICB, it appears that faults trending to the northwest of the regional orientation appear transpressional, whereas more northerly trending faults appear transtensional (e.g., un-named central ICB faults and San Diego Bay faults) (Figure 10). Several zones of transpression and transtension shown in Figure 10 illustrate the link between fault segmentation, step overs, and trend change. For example, the change in strike of the Carlsbad trend corresponds with a change to compressional features south of the Carlsbad Canyon. The faults west of the Carlsbad trend have an extensional

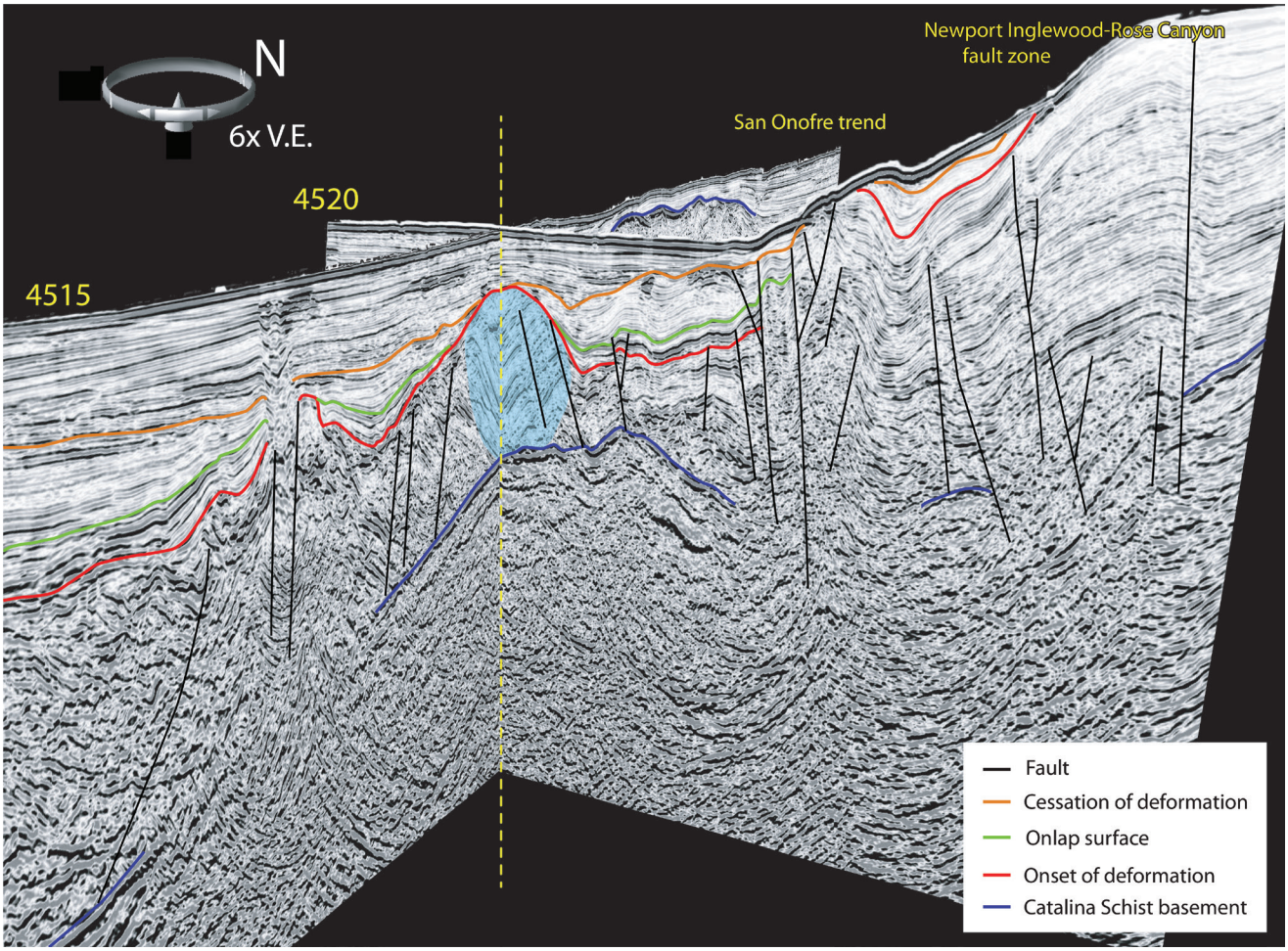

Figure 9. Fence diagram showing the reprocessed and interpreted MCS lines in a three dimensional perspective. Dashed yellow line marks the intersection between the profiles, and the shaded blue area denotes the approximate extent of the rotated block. See inset map in Figure 8 for viewing perspective (red lines). Lines 4515 and 4520 viewed from the southeast highlight the internal stratigraphy within the rotated block.

component, whereas the Carlsbad Trend and NI/RC faults appear in compression with attendant folding and uplift (Figure 6). Continuing north, the San Onofre and San Mateo trends have a more northwest strike and this change in trend corresponds to regions of deformation and uplift. Similar transpressional morphology is observed where the northerly trending unnamed faults south of Lasuen Knoll link with the more northwest trending faults associated with the Palos Verdes fault (Figure 10). As shown in the simple schematic (Figure 10), transpressional features occur at left lateral jogs along the dextral strike-slip fault systems or changes in trend to a more northwest orientation. Likewise, transtensional features are observed along right lateral jogs or changes in fault trend to a more northerly orientation.

Conclusions

Reprocessed industry MCS data place important constraints on the timing and architecture of the offshore deformation along the ICB between Dana Point, CA and the La Jolla Canyon. Any model of the offshore deformation needs to account for the following observations/results:

1. Onlapping sequences reveal that the deformation becomes younger toward the east.
2. Transport of western rotated blocks observed on MCS lines 4520, 4522, and 4515 (Figures 4, 5, 7, 8, and 9) is toward the south/southeast (Figure 10), not toward the west.
3. The Oceanside blind thrust breakaway zone is inactive and is mantled by flat-lying,

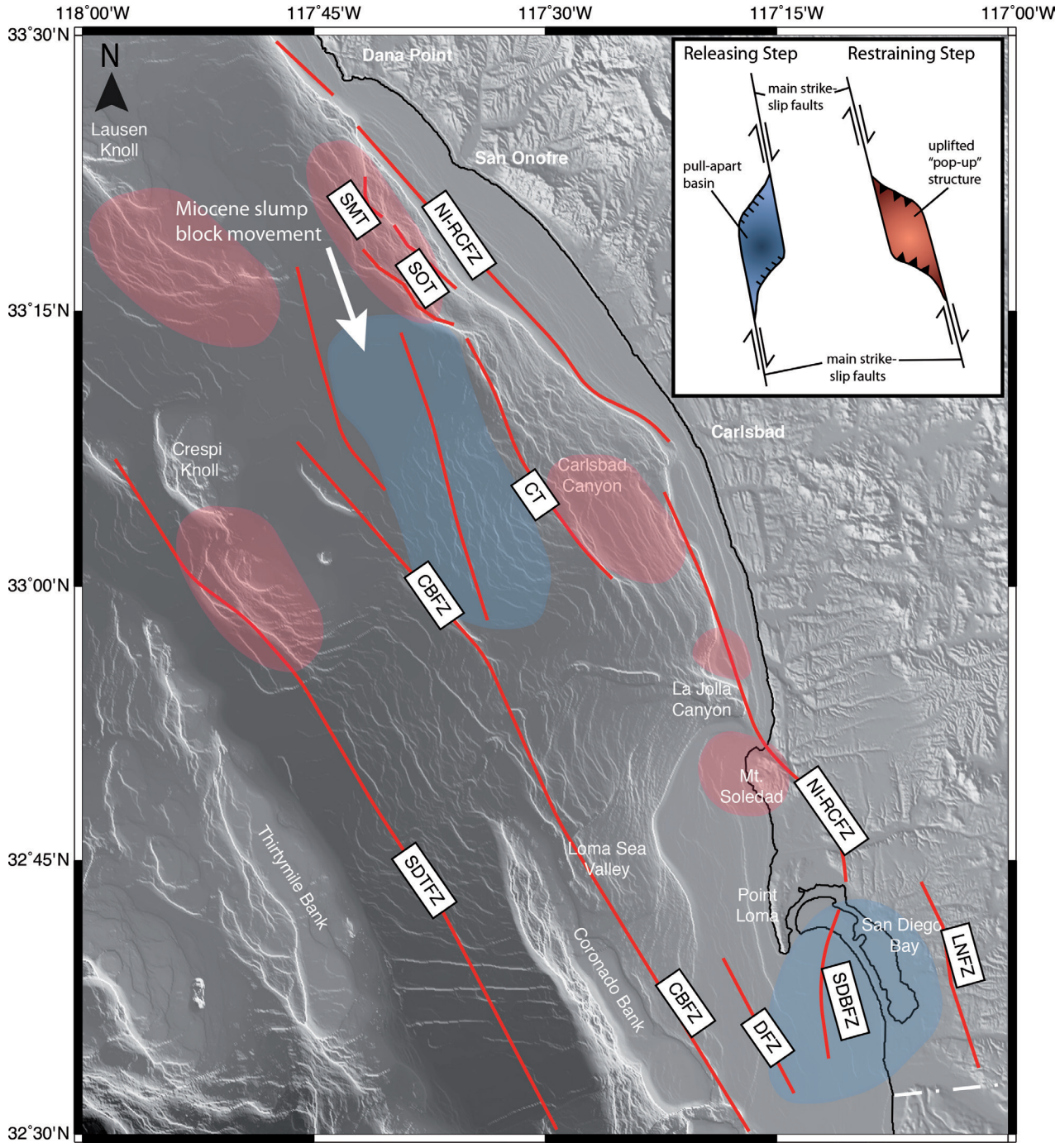

Figure 10. Map of the inner California borderlands highlighting areas of transtension (blue) and transpression (red) associated with fault bends and steps. Ryan et al. (2012) proposed transpression at a bend in the San Diego Trough fault zone south of Crespi Knoll, and Hogarth et al. (2007) reported evidence for transpression at a bend in the Rose Canyon fault zone north of La Jolla canyon. Evidence for transtension north west of La Jolla Canyon is detailed in the text, and appears to be associated with a releasing step along major strike-slip fault zones. Simple models for idealized releasing and restraining bends are illustrated in the upper right corner, as modified from Wakabayashi et al. (2004). Abbreviations: SDTFZ - San Diego Trough fault zone; CBFZ - Coronado Bank fault zone; DFZ - Descanso fault zone; LNFZ - La Nacion fault zone; NI-RCFZ - Newport Inglewood-Rose Canyon fault zone; SMT - San Mateo trend; SOT- San Onofre trend; CT - Carlsbad trend; SDBFZ - San Diego Bay faults.

onlapping reflectors of probable Pliocene age.

4. Localized compression and extension occurs as predicted at fault bends and step-overs (i.e., un-named faults).
5. The stratigraphic dip changes from a westward dip in the north (e.g., MCS line 4516, Figure 3) to an eastward dip with divergent reflectors in the south (e.g., MCS line 4542, Figure 6).
6. The lack of deformation in the Late Pliocene/Pleistocene onlapping sequences (e.g., MCS lines 4520, 4522; Figures 4 and 5) suggest deformation west of the San Mateo, San Onofre, and Carlsbad trends is old (Late Pliocene).

In summary, the timing and style of deformation observed in the ICB is better explained by strike slip fault segmentation, lateral jogs, and changes in fault trend than by a regional thrust system or a large rotating block. If correct, the hazard for coastal regions in southern California will be reduced because of two major reasons (1) there will be no potential hangingwall effects on ground motion for coastal regions associated with the OBT and (2) the slip rate predicted to occur on the purported OBT (~ 0.62 mm/yr; Field et al., 2013 – UCERF3) under the coast will not exist.

Acknowledgments

Funding for this research was provided by the National Science Foundation (OCE0649410) and a Southern California Edison grant funded through the California Public Utility Commission (CPUC). Thomas Rockwell and Paul Umhoefer provided thoughtful reviews.

REFERENCES

Anderson, J. G., Rockwell, T. K., and Agnew, D. C., 1989, Past and possible future earthquakes of significance to the San Diego Region: Earthquake Spectra, v. 5, no. 2, p. 299–335.

Astiz, L., and Shearer, P. M., 2000, Earthquake locations in the inner Continental Borderland, offshore southern California: Bulletin of the Seismological Society of America, v. 90, no. 2, p. 425–449.

Atwater, T., 1970, Implications of plate tectonics for the Cenozoic tectonic evolution of western North America: Geological Society of America Bulletin, v. 81, p. 3513–3536.

Atwater, T., and Stock, J., 1998, Pacific-North America plate tectonics of the Neogene southwestern United States: An update: International Geology Review, v. 40, no. 5, p. 375–402.

Basile, C., and Brun, J. P., 1998, Transtensional faulting patterns ranging from pull-apart basins to transform continental margins; an experimental investigation: Journal of Structural Geology, v. 21, no. 1, p. 23–37.

Becker, T. W., Hardebeck, J. L., and Anderson, G., 2005, Constraints on fault slip rates of the southern California plate boundary from GPS velocity and stress inversions: Geophysical Journal International, v. 160, no. 2, p. 634–650.

Bennett, R. A., Rodi, W., and Reilinger, R. E., 1996, Global positioning system constraints on fault slip rates in southern California and northern Baja, Mexico: Journal Of Geophysical Research, v. 101, no. B10, p. 21,943–921,960.

Boggs, S., Jr., 1995, Principles of Sedimentology and Stratigraphy, Englewood Cliffs, New Jersey, Prentice-Hall, Inc.

Bohannon, R. G., and Geist, E., 1998, Upper crustal structure and Neogene tectonic development of the California continental borderland: Geological Society of America Bulletin, v. 110, no. 6, p. 779–800.

Christie-Blick, N. and Driscoll, N. W., 1995, Sequence Stratigraphy, Annual Review of Earth and Planetary Science, v. 23, p. 451–478.

Crouch, J. K., 1979, Neogene tectonic evolution of the western Transverse Ranges and the California Continental Borderland: Geological Society of America Bulletin, v. 90, p. 338–345.

Crouch, J. K., and Bachman, S., 1989, Exploration potential of Offshore Newport-Inglewood fault zone: AAPG Bulletin, v. 73, p. 536.

Crouch, J. K., and Suppe, J., 1993, Late Cenozoic tectonic evolution of the Los Angeles Basin and inner California borderland; a model for core complex-like crustal extension: Geological Society of America Bulletin, v. 105, no. 11, p. 1415–1434.

Darigo, N. J., and Osborne, R. H., 1986, Quaternary stratigraphy and sedimentation of the inner continental shelf, San Diego County, California: Memoir - Canadian Society of Petroleum Geologists, v. 11, p. 73–98.

Dixon, T., Farina, F., DeMets, C., Suarez-Vidal, F., Fletcher, J., Marquez-Azua, B., Miller, M., Sanchez,

O., and Umhoefer, P. J., 2000, New kinematic models for Pacific-North America motion from 3 Ma to present; II, Evidence for a "Baja California shear zone": Geophysical Research Letters, v. 27, no. 23, p. 3961–3964.

Fairbanks, R. G., 1989, A 17,000-year glacio-eustatic sea level record; influence of glacial melting rates on the Younger Dryas event and deep-ocean circulation: Nature, v. 342, no. 6250, p. 637–642.

Field, E.H., Biasi, G.P., Bird, P., Dawson, T.E., Felzer, K.R., Jackson, D.D., Johnson, K.M., Jordan, T.H., Madden, C., Michael, A.J., Milner, K.R., Page, M.T., Parsons, T., Powers, P.M., Shaw, B.E., Thatcher, W.R., Weldon, R.J., II, and Zeng, Y., 2013, Uniform California earthquake rupture forecast, version 3 (UCERF3)—The time-independent model: U.S. Geological Survey Open-File Report 2013–1165, 97 p., California Geological Survey Special Report 228, and Southern California Earthquake Center Publication 1792, http://pubs.usgs.gov/of/2013/1165/.

Fischer, P. J., and Mills, G.I., 1991, The offshore Newport-Inglewood - Rose Canyon fault zone, California: structure, segmentationn and tectonics: Environmental Perils San Diego Region, San Diego Association of Geologist, p 17–36.

Freeman, T.S., Heath, E.G., Guptill, P.D., and Waggoner, J.T., 1992, Seismic hazard assessment, Newport-Inglewood fault zone, in Engineering Geology Practice in Southern California, Special Publication, no. 4, Association of Engineering Geologists, Southern California Section, p. 211–231.

Grant, L.B. and Rockwell, T.K., 2002, Northward-propagating earthquake sequence in coastal Southern California: Seismological Research Letters, v. 73, no. 2, p. 461–469.

Grant, L.B. and Shearer, P.M., 2004, Activity of the offshore Newport-Inglewood Rose Canyon fault zone, coastal southern California, from relocated microseismicity: Bulletin of the Seismological Society of America, v. 94, p. 747–752.

Hart, M. W., 1974, Radiocarbon ages of alluvium overlying La-Nacion fault, San-Diego, California: Geological Society Of America Bulletin, v. 85, no. 8, p. 1329–1332.

Henkart, P., 2003, SIOSEIS software. Scripps Institution of Oceanography, La Jolla, California. http://sioseis.ucsd.edu.

Hogarth, L. J., Babcock, J., Driscoll, N. W., Dantec, N. L., Haas, J. K., Inman, D. L., and Masters, P. M., 2007, Long-term tectonic control on Holocene shelf sedimentation offshore La Jolla, California: Geology, v. 35, no. 3, p. 275–278.

Jackson, J., and Molnar, P., 1990. Active faulting and block rotations in the western Transverse Ranges, California: Journal of Geophysical Research, v. 95, p. 22,073–22,0089.

Katzman, R., ten Brink, U. S., and Lin, J., 1995, Three-dimensional modeling of pull-apart basins; implications for the tectonics of the Dead Sea Basin: Journal of Geophysical Research, v. 100, no. B4, p. 6295–6312.

Kennedy, M. P., and Clarke, S. H., 1999, Analysis of late quaternary faulting in San Diego Bay and hazard to the Coronado Bridge: California Division of Mines and Geology Open-File Report, v. 97–10A.

Kennedy, M. P., Clarke, S. H., Greene, H. G., and Legg, M. R., 1979, Recency and character of faulting offshore from metropolitan San Diego, California: California Division of Mines and Geology, p. 37.

Kennedy, M. P., and Moore, G. W., 1971, Stratigraphic relations of upper Cretaceous and Eocene formations, San Diego coastal area, California: The American Association of Petroleum Geologists Bulletin, v. 55, no. 5, p. 709–722.

Kennedy, M. P., and Tan, S. S., 2005, Geologic Map of the San Diego 30' x 60' Quadrangle, California. Regional Geologic Map Series 1:100,000 scale, Map No. 3: California Geological Survey, California Department of Conservation.

Kennedy, M. P., Tan, S. S., Chapman, R. H., and Chase, G. W., 1975, Character and recency of faulting, San Diego Metropolitan Area, California.

Kennedy, M. P., and Welday, E. E., 1980, Recency and character of faulting offshore metropolitan San Diego, California: California Division of Mines and Geology.

Kern, J. P., and Rockwell, T. K., 1992, Chronology and deformation of Quaternary marine shorelines, San Diego County, California: Annual Field Trip Guidebook. South Coast Geological Society, v. 20, p. 1–7.

Ku, T.-L., and Kern, J. P., 1974, Uranium-Series Age of the Upper Pleistocene Nestor Terrace, San Diego, California: Geological Society of America Bulletin, v. 85, no. 11, p. 1713–1716.

Le Dantec, N., Hogarth, L. J., Driscoll, N. W., Babcock, J. M., Barnhardt, W. A., and Schwab, W. C., 2010, Tectonic controls on nearshore sediment accumulation and submarine canyon morphology offshore La Jolla, Southern California: Marine Geology, v. 268, no. 1-4, p. 115–128.

Legg, M. R., 1991. Developments in understanding the tectonic evolution of the California Borderlands, in Osbourne, R.H. ed., From shoreline to abyss: Contributions in Marine Geology in honor of Francis Parker Shepard: Tulsa Oklahoma, Society of Economic Paleontologists and mineralogists Special Publication 46:291–312.

Legg, M. R., 1985, Geologic structure and tectonics of the inner continental borderland offshore northern Baja California, Mexico: University of California Santa Barbara Ph.D. thesis.

Legg, M. R., and Kennedy, M. P., 1979, Faulting offshore San Diego and northern Baja California, in Abbott, P. L., and Elliott, W. J., eds., Earthquakes and other perils, San Diego region: San Diego, California, San Diego Association of Geologists, p. 29–46.

Lindvall, S. C., and Rockwell, T. K., 1995, Holocene activity of the Rose Canyon fault zone in San Diego, California: Journal of Geophysical Research, v. 100, no. B12, p. 24,121–124,132.

Lonsdale, P.F., 1991, Structural patterns of the Pacific floor offshore of peninsular California, in The Gulf and Peninsular Province of the Californias, AAPG Memoir, v. 47, p. 87–125.

Luyendyk, B.P., 1991, A model for the Neogene crustal rotation, transtension, and transpression in southern California, Geological Society of America Bulletin, v. 103, p. 1528–1536.

Magistrale, H., 1993, Seismicity of the Rose Canyon fault zone near San Diego, California: Bulletin of the Seismological Society of America, v. 83, no. 6, p. 1971–1978.

McClay, K., and Dooley, T., 1995, Analogue models of pull-apart basins: Geology, v. 23, no. 8, p. 711–714.

Meade, B. J., and Hager, B. H., 2005, Block models of crustal motion in Southern California constrained by GPS measurements: Journal of Geophysical Research, v. 110, no. B03403.

Moore, G. W., 1972, Offshore extension of the Rose Canyon Fault, San Diego, California: U. S. Geological Survey Professional Paper, Report: P0800C, p. 113–116.

Moore, G. W., and Kennedy, M. P., 1975, Quaternary faults at San Diego Bay, California: Journal of Research of the U. S. Geological Survey, v. 3, no. 5, p. 589–595.

Muhs, D. R., Simmons, K. R., Kennedy, G. L., and Rockwell, T. K., 2002, The last interglacial period on the Pacific Coast of North America: Timing and paleoclimate: Geological Society of America Bulletin, v. 114, no. 5, p. 569–592.

Nicholson, C., Sorlien, C. C., Atwater, T., Crowell, J. C., and Luyendyk, B. P., 1994, Microplate capture, rotation of the western Transverse Ranges, and initiation of the San Andreas transform as a low-angle fault system: Geology, v. 22, no. 6, p. 491-495.

Nilson, T. H., and Abbott, P. L., 1979, Turbidite sedimentology of the upper Creatceous Point Loma and Cabrillo Formations, San Diego, California, in Abbott, P. L., ed., Geologic excursions in the Southern California area: San Diego, California, Department of Geological Sciences, San Diego State University, p. 139–166.

Rivero, C., and Shaw, J. H., 2011, Active folding and blind thrust faulting induced by basin inversion processes, inner California borderlands, in Shaw, J. H., and Suppe, J., eds., Thrust fault related folding, Volume AAPG Memoir 94, p. 187–214.

Rivero, C., Shaw, J. H., and Mueller, K., 2000, Oceanside and Thirtymile Bank blind thrusts: Implications for earthquake hazards in coastal southern California: Geology, v. 28, no. 10, p. 891–894.

Rockwell, T., 2010, The Rose Canyon Fault Zone in San Diego, Fifth International Conference on Recent Advances in Geotechnical Earthquake Engineering and Soil Dynamics and Symposium in Honor of Professor I.M. Idriss: San Diego, California.

Ryan, H. F., Legg, M. R., Conrad, J. E., and Sliter, R. W., 2009, Recent faulting in the Gulf of Santa Catalina; San Diego to Dana Point: Special Paper - Geological Society of America, v. 454, p. 291–315.

Ryan, H. F., Conrad, J. E., Paull, C. K., and McGann, M., 2012, Slip Rate on the San Diego Trough fault zone, inner California borderland, and the 1986 Oceanside earthquake swarm revisited, Bulletin of the Seismological Society of America, v. 102, no. 6, p. 2300–2312, doi: 10.1785/0120110317.

Smith, W. H. F. and D. T. Sandwell, 1997, Global Seafloor Topography from Satellite Altimetry and Ship Depth Soundings, Science 277: 1956-1962. http://www.sciencemag.org/content/vol277/issue5334/.

Sorlien, C. C., Nicholson, C., Luyendyk, B. P., Legg, M. R., and Anonymous, 1993, Miocene collapse of the California continental margin: Abstracts with Programs - Geological Society of America, v. 25, no. 6, p. 311.

Sorlien, C., Cambell, B., Alward, W., Seeber, L., Legg, M., and Cormier, H., 2009, Transpression

in strike-slip restraining segments versus regional thrusting in the inner California Continental Borderland, Southern California Earthquake Center Annual Meeting, Proceedings and Abstracts v. XIX poster 2-026, p. 264–265.

ten Brink, U., Zhang, J., Brocher, T., Okaya, D., Klitgord, K. and Fuis, G., 2000, Geophysical evidence for the evolution of the California Inner Continental Borderland as a metamorhic core comple: Journal of Geophysical Research, v. 105, p. 5835–5857.

Treiman, J. A., 1993, The Rose Canyon Fault Zone, Southern California, California Department of Conservation, Division of Mines and Geology.

U.S. Geological Survey (USGS), 2006, National Archive of Marine Seismic Surveys: West Coast Surveys, (http://walrus.wr.usgs.gov/NAMSS/west_coast_surveys.html).

Wakabayashi, J., Hengesh, J. V., and Sawyer, T. L., 2004, Four-dimensional transform fault processes: progressive evolution of step-overs and bends: Tectonophysics, v. 392, p. 279–301.

Walls, C., Rockwell, T. K., Mueller, K., Block, Y., Williams, S., Pfanner, J., Dolan, J. F., and Fang, P., 1998, Escape tectonics in the Los Angeles metropolitan region and implications for seismic risk: Nature, v. 394, no. 6691, p. 356–360.

Wiegand, J. W., 1970, Evidence of a San Diego Bay-Tijuana Fault: Bulletin of the Association of Engineering Geologists, v. 7, no. 2, p. 107–121.

Wu, J. E., McClay, K., Whitehouse, P., and Dooley, T., 2009, 4D analogue modelling of transtensional pull-apart basins: Marine and Petroleum Geology, v. 26, no. 8, p. 1608–1623.

Dr. Jillian Maloney is an assistant professor of geology at San Diego State University. Using both geologic and geophysical datasets, Maloney seeks to understand tectonic deformation and sediment processes along continental margins. Her research has focused on offshore neotectonics, paleoseismology, and landslide dynamics in tectonically active settings. Maloney has also conducted research on marine geohazards and sediment dispersal along passive margins.

Dr. Neal Driscoll is a professor of geology and geophysics at Scripps Institution of Oceanography, University of California, San Diego. Driscoll's primary interest is in tectonic deformation and the evolution of landscapes and seascapes. His work primarily focuses on the sediment record to understand the processes that shaped the earth. Simply stated, stratigraphy is the tape recorder of Earth's history. Nevertheless, the fidelity with which stratigraphy records the dynamic processes of sediment erosion, transport, accumulation, and preservation is still incompletely understood. Although these processes can be examined from many perspectives, Driscoll's research has focused on unconformity generation and stratigraphic development in tectonically active settings and sediment input and dispersal along continental margins.

Dr. Graham Kent, Director of the Nevada Seismological Laboratory, specializes in reflection seismology, mid-ocean ridge dynamics, tectonics of the Gulf of California–Walker Lane transtentional system, Southern California tectonics, development of underwater approaches to paleoseismology, and earth science-related high end visualization. Dr. Kent also works with instrumentation, including the development of a 100-instrument ocean-bottom seismograph pool (developed at Scripps, PI), and more recently, upgrading the microwave system in eastern California and Nevada to support digital delivery of "all hazards" to include: seismic, fire and extreme weather data types.

Steve Duke is currently a Senior Project Geophysicist/Geologist with GeoPentech with over 20 years of consulting experience focused on seismic hazard assessment and geologic characterization for a wide variety of civil engineering projects. He is a California registered professional geophysicist and geologist and certified engineering geologist and hydrogeologist, and received his B.S. and M.S. degrees in Geophysics from U.C. Los Angeles and Colorado School of Mines, respectively.

Tom Freeman is a California registered professional geologist and certified engineering geologist and hydrogeologist. His 44 yrs of experience spans the geologic and seismic hazards through-out California, North America, and internationally; focused on major water, power, transportation, and military facilities in southern California. He holds a B.S. in Geology from the U.C. Santa Barbara and a M.S. in Geological Engineering from U.C. Berkeley.

Dr. Jayne Bormann is a postdoctoral research fellow at the Nevada Seismological Lab, University of Nevada, Reno. Bormann's research uses geologic and field-based geophysical techniques to study active tectonics and characterize fault systems for seismic hazard assessment. Bormann's research is primarily focused on distributed zones of deformation associated the Pacific/North American plate boundary, with current research projects in the Walker Lane and Inner California Borderlands.